Global Change Biology Communications

WILEY

Global Change Biology Communications
BIOLOGY FOR A RAPIDLY CHANGING WORLD

RESEARCH ARTICLE OPEN ACCESS

Convergent Post-Drought Recovery of Biomass and Functional Traits Under Constant and Periodic Warming in Slow- and Fast-Growing Plants

Nicolò Tartini | Ludovico Formenti | Yu Sun | Lauriane Bégué | Caroline Daniel | Itzel Lopez-Montoya | Gerard Martínez-De León | Nicholas O. E. Ofiti | Hang Zhao | Madhav P. Thakur

Institute of Ecology and Evolution, University of Bern, Bern, Switzerland

Correspondence: Madhav P. Thakur (madhav.thakur@unibe.ch)

Received: 11 November 2025 | **Revised:** 15 May 2026 | **Accepted:** 27 May 2026

Keywords: biomass-trait relationships | climate change | ecological stability | extreme drought | heat waves | invasive species

ABSTRACT

Extreme climate events such as droughts and heat waves are intensifying under climate change, yet their combined effects on plant recovery remain unclear. In a 2-year outdoor mesocosm experiment, we tested how grassland species with contrasting growth strategies recover from summer drought under four warming regimes: ambient, constant warming (+2°C), periodic heat waves (+7°C), and their combination. Experimental communities of native fast- and slow-growing species plus the invasive *Solidago canadensis* were assessed for above-ground biomass and leaf traits (SLA, LDMC, chlorophyll content, stomatal conductance) at 1 and 4 months post-drought. Biomass fully recovered within 1 month in both growth strategies, but leaf traits showed transient shifts, over-recovery in SLA and under-recovery in LDMC, likely reflecting production of new leaf tissues. These deviations generally returned to control levels by 4 months, regardless of warming treatments. *Solidago canadensis* exhibited high tolerance to heat and drought, with early biomass and trait recovery, indicating potential for dominance under climate extremes. Biomass recovery was similar across growth strategies, suggesting that growth-related differences play a minimal role in short-term recovery; however, early regrowth was characterized by contrasting trait shifts. Such lagged trait recovery, combined with rapid invasive recovery, suggests potential for longer-term shifts in grassland composition and function. We recommend that incorporating trait-based recovery dynamics is essential for predicting ecosystem stability under compound climate extremes.

1 | Introduction

Over the past few decades, the magnitude and frequency of climate extremes, such as periodic heat waves and prolonged periods of droughts are increasing at an alarming rate (IPCC 2023; Gu et al. 2025). Periodic heat waves and extreme droughts disrupt plant communities (de Boeck et al. 2011; Smith et al. 2024), such as by negatively impacting biomass productivity, tissue quality, and altering species composition and diversity (Griffin-Nolan et al. 2019; Smith et al. 2024; Thakur et al. 2022). Such community-level shifts are ultimately shaped by how individual species respond to and recover from climate-induced stresses. Yet, we know little about how periodic heat waves (short, high-intensity temperature spikes) interact with constant warming (sustained temperature increases) to shape plant responses, particularly their post-drought recovery (Li et al. 2021; Breshears et al. 2021).

Most studies have shown that constant and moderate warming increases above-ground plant biomass while also simultaneously reducing its tissue quality (Jia et al. 2025; Lin et al. 2010; Liu et al. 2022; Wan et al. 2023; Wright et al. 2001; Zhou

Nicolò Tartini and Ludovico Formenti equal contribution.

This is an open access article under the terms of the Creative Commons Attribution License, which permits use, distribution and reproduction in any medium, provided the original work is properly cited.

© 2026 The Author(s). *Global Change Biology Communications* published by John Wiley & Sons Ltd.

et al. 2022). In contrast, pulse events like periodic heat waves that are shorter in duration but higher in intensity than constant warming are typically associated with the loss in aboveground biomass productivity (Breshears et al. 2021; Wang et al. 2016), likely due to plants' inability to overcome extreme heat stress (Breshears et al. 2021; López et al. 2022; Teskey et al. 2015). Drought alone is also consistently linked with declines in plant biomass (Yu et al. 2025; Zhou et al. 2020), whereas it has been shown that interactive effects of warming and drought on plant biomass are usually additive (Wilschut et al. 2022). Indeed, the combined effects of warming and drought likely vary across species and can be effectively elucidated through trait-based approaches. For instance, species' contrasting growth strategies—fast resource acquisition versus stress tolerance—may explain their differing responses to warming and drought (Reich 2014; Wright et al. 2004; Yan et al. 2025).

Drought recovery has been shown to differ between slow- and fast-growing species (Mentges et al. 2024; Pezner et al. 2020; Prugh et al. 2018; Stotz et al. 2022). Fast-growing plants are often less drought-resistant but typically recover quickly after re-wetting (Pezner et al. 2020; Zhou et al. 2022). Conversely, slow-growing plants tend to be more resistant to climatic stressors yet recover slowly, often due to lagged responses (Prugh et al. 2018; Reich 2014; Breshears et al. 2021; Luo, Ma, et al. 2023; Zwicke et al. 2015). Such differences can be assessed via key functional traits, including chlorophyll content, stomatal conductance, specific leaf area (SLA), and leaf dry matter content (LDMC) among others (Cornelissen et al. 2003; Poorter et al. 1995; Reich 2014; Wright et al. 2004). Drought generally reduces SLA and increases LDMC (Wellstein et al. 2017; Wilcox et al. 2021), while warming may increase SLA, potentially offsetting drought-induced declines within and across species. During post-drought recovery, fast-growing plants typically restore SLA and LDMC more rapidly than slow-growing plants (Chu and Farrell 2022; de Boeck et al. 2018). Moreover, fast-growing plants also tend to lose chlorophyll quickly under stress but regain it rapidly upon rehydration, whereas many slow-growing plants maintain more stable chlorophyll levels (Chu and Farrell 2022; Luo, Shi, et al. 2023; Pezner et al. 2020; Wei et al. 2023; Zhang et al. 2021). Similar patterns occur for stomatal conductance: fast growers show sharp drought-induced declines but quick recovery, while slow growers modulate water use more effectively under drought (Li et al. 2021; Luo, Shi, et al. 2023; Valerio et al. 2022). However, the combined effects of drought and warming on these traits remain underexplored, especially regarding post-drought recovery in species with contrasting growth strategies. Emerging evidence suggests extreme heat can exacerbate drought impacts, further reducing SLA and causing prolonged physiological impairment (Tello-García et al. 2020; Wellstein et al. 2017), but it is unclear whether such compound stresses differentially constrain recovery within plant communities.

To better understand differences in post-drought recovery between slow- and fast-growing plant species, it is essential to consider recovery dynamics across the entire growing season, especially in seasonally structured ecosystems like temperate grasslands where climatic events may have temporally variable effects (Castillioni et al. 2022; de Boeck et al. 2011; Sanders et al. 2025; Zhou et al. 2022). Yet, most climate-manipulation experiments focus on peak-season measurements (Stuble et al. 2021), potentially overlooking how recovery unfolds over time (Zhou et al. 2022). Slow-growing species may resist drought stress better but exhibit delayed recovery due to inherently conservative growth strategies, while fast-growing species, though more drought-sensitive, tend to recover quickly, often with pronounced trait shifts such as changes in SLA and LDMC (Figure 1). Moreover, any subsequent climatic events like periodic heat waves during late-season recovery may further modulate these trajectories, ultimately shaping species dominance and driving community reassembly under climate change (Figure 1).

We examined post-drought recovery in experimental grassland communities composed of species with contrasting growth strategies across two full growing seasons, using an outdoor experiment that combined extreme summer drought with either constant warming, periodic heat waves, or both. Within this framework, we hypothesize that recovery dynamics would diverge between slow- and fast-growing species: fast growers would show rapid early recovery but decline over time, whereas slow growers would recover more gradually. We further predicted that warming regimes would modulate these trajectories, with constant warming facilitating recovery in both groups, while periodic heat waves would constrain it, particularly in fast growers (Figure 1). By testing these hypotheses, we assess whether gradual versus abrupt warming interacts with drought to reinforce or diminish functional differences in recovery between plant strategies.

2 | Material and Methods

2.1 | Outdoor Mesocosms

We established an outdoor experimental facility at the Hasli Ethological Station in Bern, Switzerland (46°58′01.362″ N, 7°23′50.243″ E; 490.6 m a.s.l.) to study post-drought recovery of plant communities under different warming regimes. The site has a mean annual air temperature of 9.3°C and a mean annual precipitation of 1021 mm, based on 30-year reference averages from a nearby meteorological station (Zollikofen, Bern: 46°59′26.7″ N, 7°27′50.6″ E) (MeteoSwiss 2025). The facility is located in a managed meadow and comprises the outdoor mesocosm units arranged across an area of ~250 m^2 (Figure S1a).

The outdoor mesocosms were constructed from glass fiber–reinforced plastic (GRP), with inner dimensions of 1 × 1 × 0.45 m (L × W × H). Each had 20-mm insulated polyurethane (PUR) sandwich walls and a floor made of a porous polypropylene–polyester fiber matrix that allowed slow water drainage. Mesocosms were placed 1 m apart (Figure S1b; replication described under *Climate treatments*). Each mesocosm was filled with a customized artificial soil mixture (RICOTER AG, Switzerland) replicating the physicochemical properties of mineral soil from a nearby managed meadow. The mixture comprised 40% gravel (0–32 mm), 40% vegetal earth (0–15 mm), 10% sand (0–2 mm), and 10% garden compost, forming a ~35 cm mineral layer. On top, we added a 5 cm

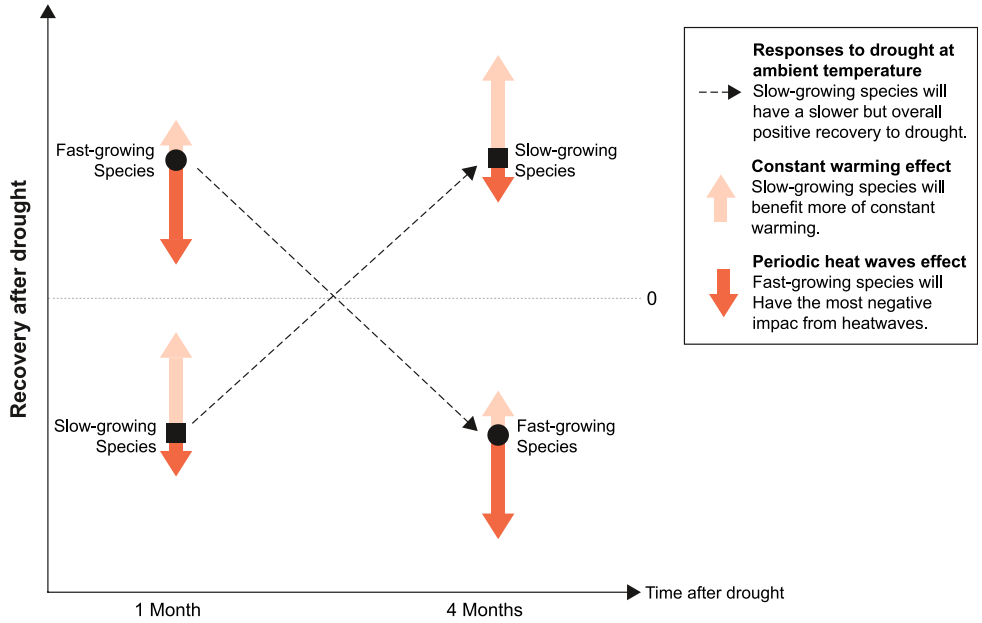


FIGURE 1 | Key hypotheses related to the responses of slow- and fast-growing plants to drought under constant and periodic warming. Plant recovery (both biomass and traits) after drought is expected to depend on growth strategy. The 1-month recovery of slow-growing species (squares) is predicted to be lower than that of fast-growing species, whereas their 4-month recovery is expected to be higher. Fast-growing species (circles) are predicted to show the opposite pattern. Warming is hypothesized to modify post-drought recovery in both strategies: Constant warming (orange arrows) is expected to enhance recovery at both stages, while periodic heat waves (dark red arrows) are expected to constrain it. The magnitude of warming effects is anticipated to differ between strategies—slow-growing species benefiting more from constant warming, and fast-growing species being more negatively affected by periodic heat waves.

layer of topsoil rich in organic matter, obtained by collecting the upper 10 cm of soil from the same meadow. The soil was sieved through a 1 cm motorized mesh (Scheppach RS 350; Scheppach GmbH, Ichenhausen, Germany) and thoroughly homogenized by hand before being added to the mesocosms. Soil properties (pH, organic matter content, and organic and inorganic C and N) were measured for the mineral- and the topsoil (Table S1). The topsoil pH was 7.21 ± 0.06 ($n = 6$) and organic matter content 29.95 ± 4.45 ($n = 2$) before plants were added (see below).

2.2 | Plant Community Establishment

In July 2022, each mesocosm was planted with an identical community of eight common grassland species characteristic of extensively managed central European meadows. Species were selected based on their position along the leaf economic spectrum (Wright et al. 2004), using specific leaf area (SLA) to represent both fast- and slow-growing strategies. To ensure phylogenetic balance, we included four plant families, each represented by one slow- and one fast-growing species: *Lotus corniculatus* (Fabaceae, slow) and *Trifolium pratense* (Fabaceae, fast); *Centaurea jacea* (Asteraceae, slow) and *Taraxacum officinale* (Asteraceae, fast); *Bromus erectus* (Poaceae, slow) and *Holcus lanatus* (Poaceae, fast); and *Salvia pratensis* (Lamiaceae, slow) and *Prunella vulgaris* (Lamiaceae, fast) (Figure 2c). Growth strategies were classified relative to other species within the same family. Alongside the native Palearctic species, we included the North American Solidago canadensis, one of the most widespread non-native invaders of central European grasslands (Nentwig et al. 2018). Note that we also added *Conyza canadensis*, another non-native species in the region, to the mesocosms at the start of the experiment, but it failed to establish and was removed from the study.

Seeds of all species were germinated indoors for 3 weeks in trays with germination soil (LANDI, Capito line) at 20°C/16°C (16 h day/8 h night) before being transplanted into a standardized randomized grid applied uniformly across all mesocosms (Figure S2). Each mesocosm received 12 individuals per species (108 plants in total). From planting until the onset of experimental treatments in March 2023, dead seedlings were regularly replaced. However, *Prunella vulgaris* failed to establish in 2022 and was therefore reintroduced during the experimental phase in spring–summer 2023.

In mid-November 2022, after plant communities had established but before the application of climatic treatments, baseline data were collected from each mesocosm (Figure S3). These data included total plant dry biomass, specific leaf area (SLA) and leaf dry matter content (LDMC). We measured specific leaf area (SLA; $mm^2\,mg^{-1}$) on young, fully expanded leaves after 24 h of water saturation on moist paper at 4°C. Leaf area was digitized using an Epson Perfection V600 Photo Scanner (Epson Corp., Nagano, Japan) (one leaf per species per mesocosm, except *L. corniculatus*, for which two leaves were sampled due to their small leaf size) and divided by leaf dry mass (dried at 70°C for 48 h). Leaf dry matter content (LDMC; $mg\,g^{-1}$) was calculated as the ratio of oven-dry mass to water-saturated fresh mass (Cornelissen et al. 2003). Once fully dried (≥ 70°C for several days), the plant material collected from each mesocosm was finely shredded and returned as litter to the same mesocosm in March 2023 to minimize



FIGURE 2 | Experimental setup. (a) A mesocosm at the onset of the drought. (b) A mesocosm with the meteorological station installed at the Hasli site. (c) Illustration of the nine study species arranged by growth strategy: *Solidago canadensis* was excluded from the fast–slow classification due to its invasive status in Europe.

nutrient loss from the system. The same procedure was repeated for plant material collected in 2023 and 2024 (details below).

2.3 | Climate Treatments

Climate treatments consisted of four warming regimes ("Ambient temperature", "Ambient + 2°C", "Ambient + periodic heat waves", and "Ambient + 2°C + periodic heat waves") fully crossed with two precipitation regimes (control water and drought). Each treatment combination was replicated five times and randomly assigned to mesocosms (Figure S1b). The 40 mesocosms were arranged in five blocks to account for wind and light variability, with each block containing one replicate of all eight climate treatments. Warming was applied using infrared heaters (VASNER SlimLine X20, 500–2000 W, 780 nm up to 1400 nm wavelength, Germany) mounted 80 cm above the soil surface of each mesocosm (Figure S4); in the ambient treatment, fake heaters were installed as controls at the same height. Air temperature (15 cm above the soil) in each mesocosm was continuously monitored with HOBO sensors (MX2201, Oneset Computer Corp., Bourne, USA), and a weather station (Oneset Computer Corp., Bourne, USA) was installed adjacent to our mesocosms to record ambient air temperature, relative humidity, solar radiation, and rainfall (2 m above the soil) (Figure S1).

The "Ambient +2°C" treatment increased air temperature by ~2°C above ambient (15 cm above the soil) throughout the growing season (mid-March to late October), starting in 2023 and repeated in 2024 (Figure S5). The "Ambient + periodic heat waves" treatment raised air temperature by ~7°C at the same height for 1 week each month, producing seven heat waves per season (Figures S4 and S6). The "Ambient +2°C + periodic heat waves" treatment combined both approaches, maintaining a + 2°C temperature throughout the growing season while adding monthly heat waves, during each heat wave week (Figure S5). The "Ambient +2°C" treatment reflects the projected global mean temperature rise by the mid-21st century under high-emission scenarios, whereas our periodic heat-wave treatments simulate regional extremes. Periodic Heat waves treatments are consistent with IPCC AR6 projections that the hottest days can warm 1.5–3 times more than the global average—resulting in anomalies approaching +6°C to 10°C for 1 week each month (Figures S4–S6) (IPCC 2023).

The drought treatment consisted of a single extreme drought event applied each experimental year (2023 and 2024), beginning in late May until the end of June. By the end of the drought period, many plants in our experiment showed severe wilting and withering suggesting that our drought regimes were representative of both hydrological and ecological extreme drought (~5–6 weeks of complete water deprivation; Figure S7). This period was chosen to simulate summer drought, which has

increased in frequency across northern Europe, including in our study region (IPCC 2023). At the end of each simulated drought, soil water content (0–10 cm depth) declined to 0%–5%, also corresponding to an "extreme drought" category according to the U.S. Drought Monitor (National Drought Mitigation Center, USDA, and NOAA; Figure S8). To maintain drought conditions and exclude confounding rainfall, all mesocosms (drought and non-drought) were covered with transparent plastic roofs during the drought period. We measured potential shading effects with a HOBO MX2202 data logger (Onset Computer Corp., Bourne, USA) equipped with a light sensor positioned near the plant canopy, which recorded a mean reduction of ~25% in light intensity relative to the same period at a nearby climate station (Figure S9). Water control mesocosms received tap water (up to twice weekly) during the drought period according to 30-year average rainfall data from the same meteorological station located at Zollikofen in Bern (46°59′26.7″ N, 7°27′50.6″ E) (MeteoSwiss 2025), using a hose with a volume counter. Outside the experimental drought period, all mesocosms were regularly watered with tap water according to the 30-year average rainfall, particularly during prolonged periods of no or insufficient precipitation as indicated by our on-site weather station. Soil water content was regularly monitored before, during, and after drought using both (i) a TDR probe (FieldScout TDR 150 Soil Moisture Meter, Spectrum Technologies Inc., Aurora, USA) for specific time point measurements per growing-season at 10 cm depth (Figure S8), and (ii) continuous sensors (GroPoint, Onset Computer Corp., Bourne, USA) at 0–15 cm and 15–30 cm depths (Figures S10 and S11).

2.4 | Plant Data Collection (2023 and 2024)

Species-specific plant data were collected prior to drought (early growing season, mid–late May), 1 month after drought (mid-July), and 4 months after drought (mid-October). To avoid re-sampling the same plant material within the same year in each mesocosm, different quarters (0.5 × 0.5 m) were randomly selected each in 2023 and 2024. Most plant-specific measurements followed the 2022 protocol, with two exceptions. First, chlorophyll content was measured with a Force-A Dualex meter (Force-A, Orsay, France). At the end of the 2024 growing season, however, we used a SPAD meter (Konica Minolta, Osaka, Japan) due to the unavailability of the Dualex. Second, we measured stomatal conductance using an SC-1 leaf porometer (Decagon Devices Inc., USA), excluding values above 500 mmol $m^{-2} s^{-1}$ because they exceed the instrument's precision range. To further illustrate the extremity of the drought treatment, we also report stomatal conductance of each species immediately after drought, before rewetting (Figure S12). Plant recovery after drought (at 1 and 4 months) was quantified for all nine species across the four warming regimes, using measurements of shoot biomass, SLA, LDMC, chlorophyll content, and stomatal conductance.

2.5 | Statistical Analysis

Post-drought plant recovery across warming regimes was analyzed separately for all response variables using R v.4.3.3 (R Core Team 2023). Mixed-effects models were fitted with the package glmmTMB v.r1.1.9 (Brooks et al. 2017). All models included the interactive effects of drought, temperature, season, and either plant growing strategies or species (see details below). Our analyses focused on post-drought responses during the peak of the growing season (1-month recovery) and the end of the growing season (4-months recovery). Since plants in spring 2023 had not yet experienced any drought, pre-drought responses (early growing season) of 2023 were not used in our mixed-effects models. Responses in spring 2024 are used in mixed-effects models as they likely reflect the legacy effects of the 2023 drought (Figure S13). Accordingly, spring 2024 data were included in the mixed-effects models (responses shown in Figure S14, Tables S3–S12). Post-drought recovery was quantified as effect sizes from the mixed-effects models.

All models included plots (to account for the repeated measurements) and year (two levels) as independent random effects. We applied two main modeling approaches. First, we tested whether slow- versus fast-growth strategies explained recovery across eight native species, with species included as a random effect to capture variation beyond growth strategy (Tables S2–S6). We considered two main growing strategies: native slow- and fast-growing species, whereas invasive species (*S. canadensis*) was used as another level. Growing all species in a shared experimental community minimized environmental variability and strengthened trait-based inference. Second, we analyzed species-specific responses by treating species as fixed effects in models that excluded growth strategy (Tables S8–S12). Models for *Prunella vulgaris* were analyzed separately due to their poor establishment in 2022 and 2023.

To ensure optimal model fit for each response variable, we applied appropriate statistical distributions and transformations. Biomass was modeled with a negative binomial distribution, except for *P. vulgaris*, where a Gaussian distribution was used. SLA and LDMC were modeled with Gaussian distributions, whereas for *P. vulgaris*, a negative binomial distribution was more appropriate. Chlorophyll content was modeled with a negative binomial distribution. Stomatal conductance was log-transformed and modeled with a Gaussian distribution, except for *P. vulgaris*, where it was again fitted with a negative binomial distribution. We tested the fit of all mixed-effects models, checking the models' residuals using the package DHARMa v.04.7 (Hartig 2016). The model assumptions were generally met, except the model for the above-ground biomass of *P. vulgaris*, which showed a poor fit (across different error distributions), and therefore, those results should be interpreted cautiously.

After fitting mixed-effects models for each response variable, we calculated drought effect sizes in all four warming treatments, using the packages emmeans v1.10.1 (Lenth and Piaskowski 2026) and effsize v0.8.1 (Torchiano 2020). Full model outputs and effect sizes are provided in the Supporting Information (Tables S3–S12). Post-drought recovery at 1 and 4 months after drought was visualized as Cohen's *d* with 95% confidence intervals (CIs) across all warming regimes. Effect sizes were plotted using the ggplot2 package (Wickham 2016). Recovery outcomes were classified as full recovery (non-significant, CI overlapping zero), under-recovery (significant negative effect), or over-recovery (significant positive effect).

3 | Results

3.1 | Growth-Strategy-Specific Recovery

Full recovery of above-ground biomass in slow- and fast-growing plants was evident already 1 month after drought across all warming treatments (Figure 3), despite clear signs of severe stress and wilting, including altered stomatal conductance recorded immediately post-drought (Figures S7 and S12). This full biomass recovery persisted 4 months after drought in both growth strategies and across warming treatments (Figure 3).

By contrast, we found pronounced shifts in SLA and LDMC 1 month after drought across warming regimes. SLA showed significant over-recovery, increasing on average by 26.1% in slow-growing species and 18.6% in fast-growing species compared with water controls. Reciprocally, LDMC showed significant under-recovery, with decreases of 19.4% in slow-growing species and 17.5% in fast-growing species. Differences between growth strategies were not statistically significant for either of the traits (Tables S3–S7). By 4 months after drought, both SLA and LDMC fully recovered across warming regimes and growth strategies, with the sole exception of SLA in fast-growing species under constant warming, which remained above control levels (Figure 3).

3.2 | Species-Specific Recovery

All eight native species almost fully recovered in biomass and functional traits 4 months after drought; however, distinct differences in recovery emerged more clearly 1 month after drought, particularly in the warmed treatments (Figure 4). Interestingly, *T. pratense* was the only species to show under-recovery in above-ground biomass 4 months post-drought under constant warming, despite its earlier over-recovery in the same treatment just 1 month after drought (Figure 4). Indeed, many species (*B. erectus*, *T. pratense*, *T. officinale*, and *P. vulgaris*) showed the pattern of over-recovery 1 month after drought, and periodic heat waves contributed to this pattern in *B. erectus*, *T. pratense*, and *T. officinale*.

Traits related to photosynthesis and gas exchange, namely chlorophyll content and stomatal conductance, also reached full-recovery in most species after 1 month of drought across warming regimes (Figure 4). By contrast, traits related to leaf tissue quality (SLA, LDMC) showed over- or under-recovery in many species 1 month after drought, and even persisted in a few cases 4 months (e.g., *H. lanatus*) after the extreme drought event. The LDMC in *B. erectus*, *C. jacea*, *S. pratensis*, *H. lanatus*, *T. pratense* was under-recovering 1 month after drought, and notably so in constantly warmed treatments (Figure 4). The combined constant and periodic heat wave treatments ("Ambient + 2°C + periodic heat waves") further amplified the under-recovery in *C. jacea* at this time point of post-drought recovery. Interestingly, *C. jacea* showed over-recovery in its biomass 4 months after drought under the same intensified warming regime (Figure 4). In addition, many species showed an inverse recovery pattern between SLA and LDMC, with SLA frequently over-recovering in cases where LDMC was under-recovering (Figure 4). Most cases of SLA over-recovery 1 month after drought converged to full recovery by 4 months, except for *H. lanatus*, where SLA values remained high under both constant warming and periodic heat wave treatments.

The invasive species *S. canadensis* in our experimental plant community was largely tolerant to drought and showed a rapid recovery to both drought and warming, with a few notable exceptions. For instance, it showed a significant decline (under-recovery) in LDMC 4 months after drought, despite no change 1 month post-drought (Figure 4). Moreover, its stomatal conductance exhibited under-recovery 1 month after drought under the combined constant warming and periodic heat waves (Figure 4).

4 | Discussion

Using an outdoor experiment over two consecutive growing seasons, we found that several common temperate grassland species achieved full post-drought recovery under both constant warming and periodic heat waves. More strikingly, by 4 months after extreme drought—coinciding with the end of the growing season—both slow- and fast-growing species reached full recovery, regardless of warming and even sharing the same recovery trajectories in both 1 and 4 months post drought data points. These findings contradict our hypothesis, which predicted a delayed recovery in slow-growing species and a faster recovery in fast-growing species (Figure 1).

Both fast- and slow-growing species recovered their biomass at similar rates under all warming regimes, suggesting that the severity of the drought was so intense that it forced plants to pursue the same recovery mechanisms, equalizing their responses. We suspect that extreme water limitation may have created a threshold condition, forcing plants into a common "stasis" response characterized by halted growth and canopy dieback (Breshears et al. 2021). Upon rewetting during the peak of the growing season (e.g., July), when light and temperature conditions are optimal, plants rapidly regenerated above-ground tissues to ensure survival through the remainder of the season (Zhou et al. 2022). The mechanism underlying this convergence likely involved drought-induced dormancy, consistent with the absence of systematic differences in stomatal conductance between fast- and slow-growing plants under extreme drought. Non-structural carbohydrates (NSCs) accumulated prior to drought and mobilized during drought may have sustained plants through this shared dormancy state and subsequently fuelled the rapid above-ground regeneration observed upon rewetting, a mechanistic link that warrants direct investigation in future work (Wang and Wang 2025; Martínez-Vilalta et al. 2016). This convergence in recovery, rather than the expected divergence based on growth rate (Jia et al. 2025; Stuble et al. 2021), highlights the adaptive capacity of grassland species to rebound from compound stress events, and aligns with recent evidence that phenotypic plasticity under extreme events may buffer against anticipated trade-offs (Wan et al. 2023). Therefore, while our results suggest convergent post-drought recovery among the studied species, we caution against generalizing this pattern across slow- and fast-growing plant strategies, as our species

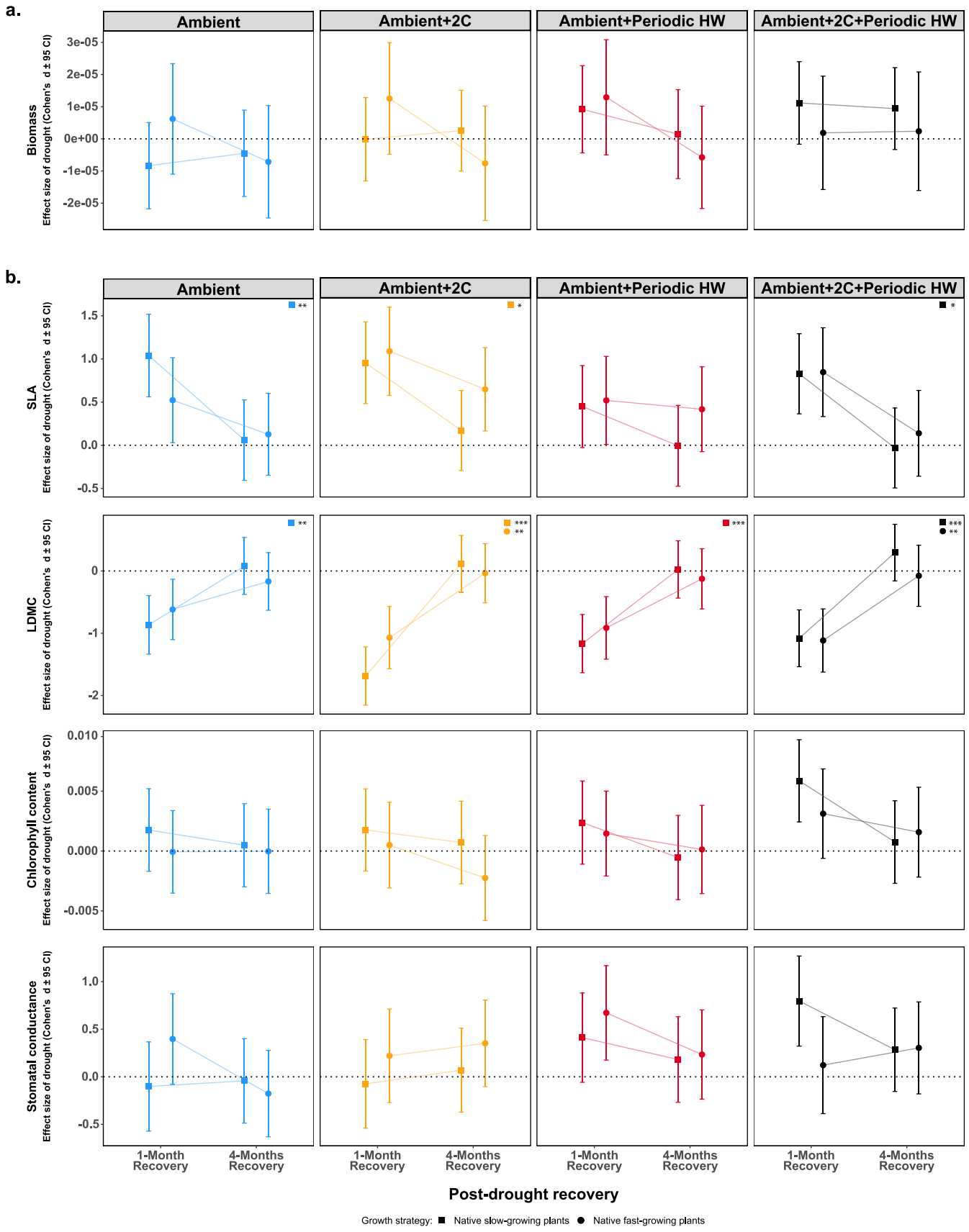


FIGURE 3 | Legend on next page.

FIGURE 3 | Post-drought recovery of slow- and fast-growing native plants 1 and 4 months after drought under four temperature regimes. Recovery is shown for shoot biomass, specific leaf area (SLA), leaf dry matter content (LDMC), chlorophyll content, and stomatal conductance, based on data from 2023 and 2024 (see Section 2). Values represent Cohen's d ±95% confidence intervals (CIs); recovery is significant when CIs do not overlap zero. Significant differences between effect sizes of the two recovery periods within each growth strategy were assessed using estimated marginal means from mixed-effects models with Tukey-adjusted pairwise comparisons (*$p < 0.05$; **$p < 0.01$; ***$p < 0.001$). HW denotes periodic heat waves. Post drought recovery is also shown as log response ratios in Figure S16.

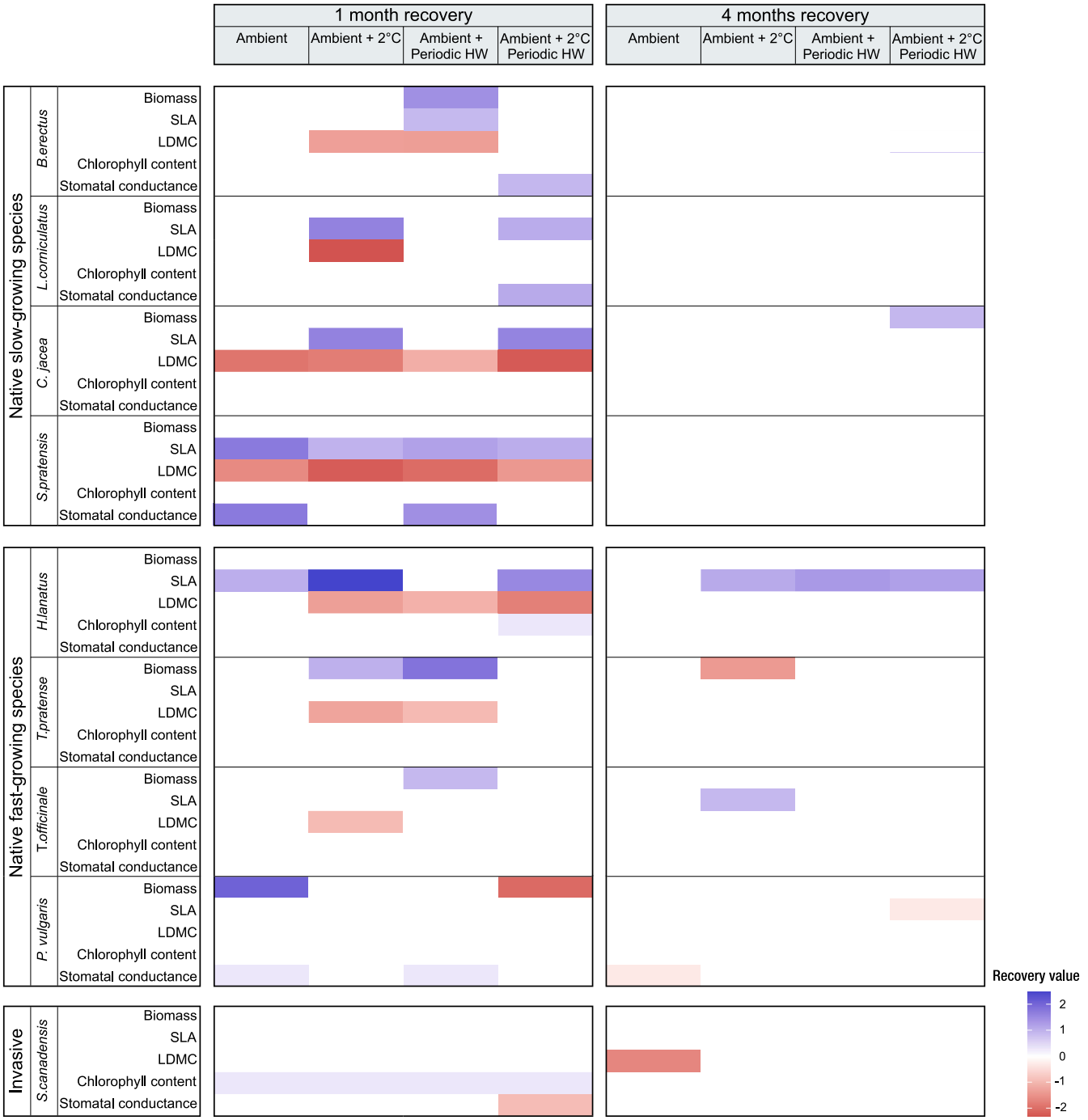


FIGURE 4 | Overview of post-drought recovery (1 and 4 months after drought) across plant species under four temperature regimes. Recovery values are expressed as effect sizes (Cohen's d). Negative values indicate under-recovery (negative drought effects; confidence intervals not overlapping zero), values around zero indicate full recovery (no difference between drought and non-drought treatments; confidence intervals overlapping zero), and positive values indicate over-recovery (positive drought effects; confidence intervals not overlapping zero). Legacy effects of the 2023 drought across warming regimes (measured in spring 2024, before the 2024 drought) are shown in Figure S13.

set does not fully capture variation along the leaf economics spectrum (Table S2).

Despite the rapid biomass recovery, leaf trait recovery suggests a more nuanced adaptive strategy of plants under drought and warming. Most species exhibited over-recovery in specific leaf area (SLA) and under-recovery in leaf dry matter content (LDMC) 1 month after drought, indicating the production of softer, less lignified foliage—traits typically associated with rapid regrowth rather than full functional recovery (Künzi et al. 2025; Wellstein et al. 2017). These patterns likely reflect the presence of young, newly formed tissues that had not yet matured structurally. By 4 months post-drought, however, most species exhibited full recovery in both SLA and LDMC, suggesting that trait-based recovery may lag behind biomass recovery. These findings underline the importance of temporal scale in interpreting the stability of plant species: apparent recovery at one functional level (biomass) may mask delays or vulnerabilities in other dimensions (tissue structure). Moreover, biomass-trait decoupling at the early recovery phase can have ecosystem-level consequences: the transient production of soft, nutrient-rich foliage may elevate herbivore pressure (Hrubá et al. 2022; Blumenthal et al. 2020) and accelerate litter decomposition (Pakeman et al. 2011), pulsing labile carbon and nutrients into the soil at a time when plants are least structurally defended—effects likely to intensify under increasingly frequent drought-rewetting cycles.

The invasive species *Solidago canadensis* showed a notable exception in our study. While largely unresponsive in biomass across treatments, *S. canadensis* exhibited under-recovery in LDMC 4 months post-drought, and its stomatal conductance was reduced 1 month after drought under the intensified warming ("Ambient + 2°C + periodic heat waves"). This response is striking if we compare it with the native species, which under the same warming condition showed a neutral or an increase in gas exchanges. The negative effect on stomatal conductance of *S. canadensis* could be a sign of a water parsimony strategy. Remarkably, *S. canadensis* partially retained above-ground foliage during drought when most native species had wilted (Figures S7 and S12), possibly enabling faster regrowth from residual tissues or rhizome reserves. Moreover, belowground plasticity and rhizomatous recovery capacity may also have contributed to its drought tolerance (Du et al. 2019). Consistent with this, the biomass of *S. canadensis* interacted significantly with drought to modulate native species LDMC recovery at 1 month of rewetting, with the direction of this relationship turning negative under warmed conditions relative to ambient (Figure S15), suggesting that the competitive influence of *S. canadensis* on native species recovery could intensify under compound climate stress. We suspect that these patterns provide *S. canadensis* with a relative advantage over native plants in extreme climatic conditions, reinforcing concerns that climate change may amplify invasive species dominance in temperate grasslands (Prugh et al. 2018; Sanders et al. 2025). In line with this, our observation that *S. canadensis* has increased its biomass dominance over 2 years in all control mesocosms (Figures S3 and S14) further suggests that such traits may shift community trajectories over time, particularly when coupled with ecosystem disturbances (Griffin-Nolan et al. 2019; Luo, Shi, et al. 2023).

Taken together, our findings highlight the strong stability of temperate grassland species to extreme drought events even under different warming regimes, particularly when conditions for regrowth are favorable. The rapid recovery of biomass and, to a slightly delayed extent, leaf traits suggests that grassland ecosystems may retain functional resilience under recurrent climate extremes—at least in the short term, as our results are based on 2 years of observation. However, this does not imply that grasslands remain unaffected: our mesocosms represent a young, still-establishing community dominated by an invasive species, and results may change as biotic interactions may lead to ecological debts under harsh and repeated abiotic conditions (Martínez-De León and Thakur 2024; Thakur et al. 2022). Furthermore, we have focused here on the above-ground plant responses. Yet, post-drought dynamics of below-ground responses, such as root biomass and traits, soil microbes and invertebrate communities, remain poorly understood and could feedback on longer-term ecosystem stability. Continued long-term monitoring is therefore essential to capture delayed effects, including potential shifts in species dominance, loss of diversity, and biogeochemical feedbacks that may only become evident over extended timescales.

Author Contributions

Nicolò Tartini: formal analysis, investigation, methodology, visualization, writing – original draft, writing – review and editing, data curation, validation. **Yu Sun:** data curation, writing – review and editing, methodology. **Nicholas O. E. Ofiti:** methodology, writing – review and editing. **Lauriane Bégué:** data curation, writing – review and editing. **Ludovico Formenti:** methodology, formal analysis, validation, visualization, investigation, writing – review and editing, writing – original draft, data curation, project administration. **Gerard Martínez-De León:** data curation, formal analysis, writing – review and editing, methodology. **Caroline Daniel:** writing – review and editing, data curation, methodology. **Itzel Lopez-Montoya:** data curation, writing – review and editing, methodology. **Hang Zhao:** data curation, methodology, writing – review and editing. **Madhav P. Thakur:** conceptualization, methodology, data curation, investigation, validation, formal analysis, supervision, funding acquisition, writing – original draft, writing – review and editing, project administration, resources.

Acknowledgments

We thank Bruno Kampf and Erich Fuhrer from the Betrieb & Technik department of the University of Bern for their support in establishing the outdoor mesocosm experiment. We are also grateful to all current and former members of the Terrestrial Ecology Group and the Institute of Ecology & Evolution for their help in setting up the experiment in 2022. Figure 1 was drawn by Nadine Kamber (https://www.definitivdesign.ch/). We further thank Philippe Graber, Anouk Gremion, Loraine Hablützel, Arianne Marty, Dennis Loosli, Johan-Jakob Schindler, Felix Rentschler, Anine Wyser, and Roem Yesil for their assistance with data collection. We acknowledge the use of Open AI ChatGPT for the language and coding refinements. We finally thank the anonymous reviewer for several constructive suggestions. This project was funded by the Swiss State Secretariat for Education, Research and Innovation (SERI) under contract number M822.00029. Open access publishing facilitated by Universitat Bern, as part of the Wiley - Universitat Bern agreement via the Consortium Of Swiss Academic Libraries.

Funding

This work was supported by Staatssekretariat für Bildung, Forschung und Innovation (M822.00029).

Conflicts of Interest

The authors declare no conflicts of interest.

Data Availability Statement

Data and codes used in this paper are available at Zenodo (https://doi.org/10.5281/zenodo.20508062).

References

Blumenthal, D. M., K. E. Mueller, J. A. Kray, T. W. Ocheltree, D. J. Augustine, and K. R. Wilcox. 2020. "Traits Link Drought Resistance With Herbivore Defence and Plant Economics in Semi-Arid Grasslands: The Central Roles of Phenology and Leaf Dry Matter Content." *Journal of Ecology* 108: 2336–2351.

Breshears, D. D., J. B. Fontaine, K. X. Ruthrof, et al. 2021. "Underappreciated Plant Vulnerabilities to Heat Waves." *New Phytologist* 231: 32–39.

Brooks, M. E., K. Kristensen, K. J. van Benthem, et al. 2017. "glmmTMB Balances Speed and Flexibility Among Packages for Zero-inflated Generalized Linear Mixed Modeling." *R Journal* 9: 378–400.

Castillioni, K., G. S. Newman, L. Souza, and A. M. Iler. 2022. "Effects of Drought on Grassland Phenology Depend on Functional Types." *New Phytologist* 236: 1558–1571.

Chu, H.-H., and C. Farrell. 2022. "Fast Plants Have Water-Use and Drought Strategies That Balance Rainfall Retention and Drought Survival on Green Roofs." *Ecological Applications* 32: e02486.

Cornelissen, J. H., S. Lavorel, E. Garnier, et al. 2003. "A Handbook of Protocols for Standardised and Easy Measurement of Plant Functional Traits Worldwide." *Australian Journal of Botany* 51: 335–380.

de Boeck, H. J., F. E. Dreesen, I. A. Janssens, and I. Nijs. 2011. "Whole-System Responses of Experimental Plant Communities to Climate Extremes Imposed in Different Seasons." *New Phytologist* 189: 806–817.

de Boeck, H. J., E. Hiltbrunner, M. Verlinden, S. Bassin, and M. Zeiter. 2018. "Legacy Effects of Climate Extremes in Alpine Grassland." *Frontiers in Plant Science* 9: 1586.

Du, L., H. Liu, W. Guan, J. Li, and J. Li. 2019. "Drought Affects the Coordination of Belowground and Aboveground Resource-Related Traits in *Solidago canadensis* in China." *Ecology and Evolution* 9: 9948–9960.

Griffin-Nolan, R. J., D. M. Blumenthal, S. L. Collins, et al. 2019. "Shifts in Plant Functional Composition Following Long-Term Drought in Grasslands." *Journal of Ecology* 107: 2133–2148.

Gu, L., D. L. Schumacher, E. M. Fischer, et al. 2025. "Flash Drought Impacts on Global Ecosystems Amplified by Extreme Heat." *Nature Geoscience* 18: 709–715.

Hartig, F. 2016. "DHARMa: Residual Diagnostics for Hierarchical Multi-Level/Mixed Regression Models." R Package. https://CRAN.R-project.org/package=DHARMa.

Hrubá, K., A. Lisner, and J. Lepš. 2022. "Effects of Phylogeny, Traits, and Seasonality on Invertebrate Herbivory Damage in a Meadow Community." *Acta Oecologica* 117: 103871.

IPCC. 2023. *Climate Change 2021: The Physical Science Basis. Working Group I Contribution to the Sixth Assessment Report of the Intergovernmental Panel on Climate Change*. Cambridge University Press.

Jia, P., R. Zhang, B. Schmid, et al. 2025. "A Global Synthesis of How Plants Respond to Climate Warming From Traits to Fitness." *Ecology Letters* 28: e70114.

Künzi, Y., M. Zeiter, M. Fischer, and A. Stampfli. 2025. "Rooting Depth and Specific Leaf Area Modify the Impact of Experimental Drought Duration on Temperate Grassland Species." *Journal of Ecology* 113: 445–458.

Lenth, R. V., and J. Piaskowski. 2026. "emmeans: Estimated Marginal Means, aka Least-Squares Means." *R package version 2.0.3*. https://rvlenth.github.io/emmeans/.

Li, L., Z. Zheng, J. A. Biederman, et al. 2021. "Drought and Heat Wave Impacts on Grassland Carbon Cycling Across Hierarchical Levels." *Plant, Cell & Environment* 44: 2402–2413.

Lin, D., J. Xia, and S. Wan. 2010. "Climate Warming and Biomass Accumulation of Terrestrial Plants: A Meta-Analysis." *New Phytologist* 188: 187–198.

Liu, H., H. Wang, N. Li, et al. 2022. "Phenological Mismatches Between Above- and Belowground Plant Responses to Climate Warming." *Nature Climate Change* 12: 97–102.

López, R., J. A. Ramírez-Valiente, and P. Pita. 2022. "How Plants Cope With Heatwaves in a Drier Environment." *Flora* 295: 152148.

Luo, W., W. Ma, L. Song, et al. 2023. "Compensatory Dynamics Drive Grassland Recovery From Drought." *Journal of Ecology* 111: 1281–1291.

Luo, W., Y. Shi, K. Wilkins, et al. 2023. "Plant Traits Modulate Grassland Stability During Drought and Post-Drought Periods." *Functional Ecology* 37: 2611–2620.

Martínez-De León, G., and M. P. Thakur. 2024. "Ecological Debts Induced by Heat Extremes." *Trends in Ecology & Evolution* 39: 1024–1034.

Martínez-Vilalta, J., A. Sala, D. Asensio, et al. 2016. "Dynamics of Non-Structural Carbohydrates in Terrestrial Plants: A Global Synthesis." *Ecological Monographs* 86: 495–516.

Mentges, A., A. T. Clark, S. A. Blowes, C. Kunze, H. Hillebrand, and J. M. Chase. 2024. "Accounting for Effects of Growth Rate When Measuring Ecological Stability in Response to Pulse Perturbations." *Ecology and Evolution* 14: e11637.

MeteoSwiss. 2025. *Climate Climsheet: Climate Reports for Bern/Zollikofen, 1991–2020*. Federal Office of Meteorology and Climatology MeteoSwiss.

Nentwig, W., S. Bacher, S. Kumschick, P. Pyšek, and M. Vilà. 2018. "More Than '100 Worst' Alien Species in Europe." *Biological Invasions* 20: 1611–1621.

Pakeman, R. J., A. Eastwood, and A. Scobie. 2011. "Leaf Dry Matter Content as a Predictor of Grassland Litter Decomposition: A Test of the 'Mass Ratio Hypothesis'." *Plant and Soil* 342: 49–57.

Pezner, A. K., A. L. Pivovaroff, W. Sun, M. R. Sharifi, P. W. Rundel, and U. Seibt. 2020. "Plant Functional Traits Predict the Drought Response of Native California Plant Species." *International Journal of Plant Sciences* 181: 256–265.

Poorter, H., C. A. van de Vijver, R. G. Boot, and H. Lambers. 1995. "Growth and Carbon Economy of a Fast-Growing and a Slow-Growing Grass Species as Dependent on Nitrate Supply." *Plant and Soil* 171: 217–227.

Prugh, L. R., N. Deguines, J. B. Grinath, et al. 2018. "Ecological Winners and Losers of Extreme Drought in California." *Nature Climate Change* 8: 819–824.

R Core Team. 2023. *R: A Language and Environment for Statistical Computing*. R Foundation for Statistical Computing.

Reich, P. B. 2014. "The World-Wide 'Fast–Slow' Plant Economics Spectrum: A Traits Manifesto." *Journal of Ecology* 102: 275–301.

Sanders, S. K., M. van Kleunen, E. Allan, and M. P. Thakur. 2025. "Effects of Extreme Drought on the Invasion Dynamics of Non-Native Plants." *Trends in Plant Science* 30: 291–300.

Smith, M. D., K. D. Wilkins, M. C. Holdrege, et al. 2024. "Extreme Drought Impacts Have Been Underestimated in Grasslands and

Shrublands Globally." *Proceedings of the National Academy of Sciences of the United States of America* 121: e2309881120.

Stotz, G. C., C. Salgado-Luarte, V. M. Escobedo, F. Valladares, and E. Gianoli. 2022. "Phenotypic Plasticity and the Leaf Economics Spectrum: Plasticity Is Positively Associated With Specific Leaf Area." *Oikos* 2022: e09342.

Stuble, K. L., L. D. Bennion, and S. E. Kuebbing. 2021. "Plant Phenological Responses to Experimental Warming: A Synthesis." *Global Change Biology* 27: 4110–4124.

Tello-García, E., L. Huber, G. Leitinger, et al. 2020. "Drought- and Heat-Induced Shifts in Vegetation Composition Impact Biomass Production and Water Use of Alpine Grasslands." *Environmental and Experimental Botany* 169: 103921.

Teskey, R., T. Wertin, I. Bauweraerts, M. Ameye, M. A. McGuire, and K. Steppe. 2015. "Responses of Tree Species to Heat Waves and Extreme Heat Events." *Plant, Cell & Environment* 38: 1699–1712.

Thakur, M. P., A. C. Risch, and W. H. van der Putten. 2022. "Biotic Responses to Climate Extremes in Terrestrial Ecosystems." *iScience* 25: 104559.

Torchiano, M. 2020. "effsize: Efficient Effect Size Computation." R Package. https://CRAN.R-project.org/package=effsize.

Valerio, M., R. Ibáñez, A. Gazol, and L. Götzenberger. 2022. "Long-Term and Year-To-Year Stability and Its Drivers in a Mediterranean Grassland." *Journal of Ecology* 110: 1174–1188.

Wan, L., G. Liu, H. Cheng, S. Yang, Y. Shen, and X. Su. 2023. "Global Warming Changes Biomass and C:N:P Stoichiometry of Different Components in Terrestrial Ecosystems." *Global Change Biology* 29: 7102–7116.

Wang, D., S. A. Heckathorn, K. Mainali, and R. Tripathee. 2016. "Timing Effects of Heat Stress on Plant Ecophysiological Characteristics and Growth." *Frontiers in Plant Science* 7: 1629.

Wang, Z., and C. Wang. 2025. "Dynamics of Nonstructural Carbohydrates During Drought and Subsequent Recovery: A Global Meta-Analysis." *Agricultural and Forest Meteorology* 363: 110429.

Wei, B., D. Zhang, G. Wang, et al. 2023. "Experimental Warming Altered Plant Functional Traits and Their Coordination in a Permafrost Ecosystem." *New Phytologist* 240: 1802–1816.

Wellstein, C., P. Poschlod, A. Gohlke, et al. 2017. "Effects of Extreme Drought on Specific Leaf Area of Grassland Species: A Meta-Analysis of Experimental Studies in Temperate and Sub-Mediterranean Systems." *Global Change Biology* 23: 2473–2481.

Wickham, H. 2016. *ggplot2: Elegant Graphics for Data Analysis*. Springer-Verlag.

Wilcox, K. R., D. M. Blumenthal, J. A. Kray, et al. 2021. "Plant Traits Related to Precipitation Sensitivity of Species and Communities in Semiarid Shortgrass Prairie." *New Phytologist* 229: 2007–2019.

Wilschut, R. A., J. R. De Long, S. Geisen, et al. 2022. "Combined Effects of Warming and Drought on Plant Biomass Depend on Plant Woodiness and Community Type: A Meta-Analysis." *Proceedings of the Royal Society B: Biological Sciences* 289: 20221178.

Wright, I. J., P. B. Reich, and M. Westoby. 2001. "Strategy Shifts in Leaf Physiology, Structure and Nutrient Content Between Species of High- and Low-Rainfall and High- and Low-Nutrient Habitats." *Functional Ecology* 15: 423–434.

Wright, I. J., P. B. Reich, M. Westoby, et al. 2004. "The Worldwide Leaf Economics Spectrum." *Nature* 428: 821–827.

Yan, P., N. He, M. Fernández-Martínez, et al. 2025. "Plant Acquisitive Strategies Promote Resistance and Temporal Stability of Semiarid Grasslands." *Ecology Letters* 28: e70110.

Yu, Q., C. Xu, H. Wu, et al. 2025. "Contrasting Drought Sensitivity of Eurasian and North American Grasslands." *Nature* 639: 114–118.

Zhang, Y., N. He, and G. Yu. 2021. "Opposing Shifts in Distributions of Chlorophyll Concentration and Composition in Grassland Under Warming." *Scientific Reports* 11: 15736.

Zhou, H., L. Hou, X. Lv, G. Yang, Y. Wang, and X. Wang. 2022. "Compensatory Growth as a Response to Post-Drought in Grassland." *Frontiers in Plant Science* 13: 1004553.

Zhou, L., Y. Hong, C. Li, et al. 2020. "Responses of Biomass Allocation to Multi-Factor Global Change: A Global Synthesis." *Agriculture, Ecosystems & Environment* 304: 107115.

Zwicke, M., C. Picon-Cochard, A. Morvan-Bertrand, M.-P. Prud'homme, and F. Volaire. 2015. "What Functional Strategies Drive Drought Survival and Recovery of Perennial Species From Upland Grassland?" *Annals of Botany* 116: 1001–1015.

Supporting Information

Additional supporting information can be found online in the Supporting Information section. **Figure S1:** (a) Aerial view of the 40 mesocosms (~250 m^2). (b) Schematic representation of the randomized treatment assignment. **Figure S2:** Schematic showing the initial planting arrangement of 12 individuals per species (represented by different colors) within each mesocosm. **Figure S3:** Baseline plant specific biomass (a) and traits (b–d) measured at the end of the growing season in 2022, a year before the climate treatments were applied. **Figure S4:** Example of the infrared heater setup. **Figure S5:** Warming treatment temperature measurements taken 15 cm above the soil surface (sensors were placed at the center of each mesocosm directly beneath the infrared heater). **Figure S6:** Δ temperature between the extreme heat-wave treatment and ambient conditions. **Figure S7:**. Images of four mesocosms at the start and end of the drought periods in 2023 and 2024, illustrating visible differences in canopy cover and plant condition. **Figure S8:** Volumetric soil water content (mean ± SE, %) under four warming treatments, measured with TDR at specific time points during the growing season: (a) Ambient (blue), (b) Ambient +2°C (orange), (c) Ambient + periodic heat waves (red), and (d) Ambient +2°C + periodic heat waves (black). **Figure S9:** Proportion of light (mean ± SE) intercepted by the roof structure placed over mesocosms during the experimental drought period. **Figure S10:** Monthly soil water content at two depths during the 2024 experimental year. **Figure S11:** Temporal dynamics of soil moisture at two depths during the 2024 growing season. **Figure S12:** Stomatal conductance (mean ± SE) measured on the final day of the drought treatment (data pooled across 2023 and 2024, except for *Prunella vulgaris*). **Figure S13:** Effect size of different warming regimes across all plants before the drought event of 2024 (2023 drought legacy effect of on plant performance in 2024 spring). **Figure S14:** Average aboveground biomass per species and year, and biomass dynamics across the 2 years of data collection. **Figure S15:** Effect of *Solidago canadensis* biomass on native plant leaf dry matter content (LDMC) during post-drought recovery. **Figure S16:** Post-drought recovery (log response ratio) of slow- and fast-growing native plants 1 and 4 months after drought under four temperature regimes. **Table S1:** Initial soil parameters (mean ± SD) for the three soil categories used in the experiment. **Table S2:** Leaf traits average value (mean ± SD) values of the studied plant species. **Table S3:** Output of the mixed-effects models testing plant biomass responses to treatments and season across different growth strategies (growth-strategy-specific recovery model). **Table S4:** Output of the mixed-effects models testing plant SLA to treatments and season across different growth strategies (growth-strategy-specific recovery model). **Table S5:** Output of the mixed-effects models testing plant LDMC responses to treatments and season across different growth strategies (growth-strategy-specific recovery model). **Table S6:** Output of the mixed-effects models testing plant chlorophyll content responses to treatments and season across different growth strategies (growth-strategy-specific recovery model). **Table S7:** Output of the mixed-effects model testing plants' stomatal conductance responses to treatments and season across different growth strategies

(growth-strategy-specific recovery model). **Table S8a:** Output of the mixed-effects models testing specific plant biomass responses to treatments and season (species-specific recovery model). **Table S8b:** Output of the general model of aboveground biomass responses to treatments and season for *Prunella vulgaris*. **Table S9a:** Output of the mixed-effects models testing specific SLA to treatments and season (species-specific recovery model). **Table S9b:** Output of the general model of the SLA responses to the treatment and season according to the plants' species *Prunella vulgaris*. **Table S10a:** Output of the mixed-effects models testing specific LDMC responses to treatments and season (species-specific recovery model). **Table S10b:** Output of the general model of the LDMC responses to the treatment and season according to the plants' species *Prunella vulgaris*. **Table S11a:** Output of the mixed-effects models testing specific chlorophyll content responses to treatments and season (species-specific recovery model). **Table S11b:** Output of the general model of the chlorophyll content responses to the treatment and season according to the plants' species *Prunella vulgaris*. **Table S12a:** Output of the mixed-effects models testing specific stomatal conductance responses to treatments and season (species-specific recovery model). **Table S12b:** Output of the general model of the stomatal conductance responses to the treatment and season according to the plants' species *Prunella vulgaris*.